

Computational Fluid Dynamics Analysis of Radiative Heat Loading on Hyper Velocity Re-Entry Vehicles

N.Vairamuthu

M.Tech Scholar

Department of Aerospace

Malla Reddy College of Engineering and Technology, Maisammaguda, Hyderabad, Telangana, India

Abstract- Space exploration missions may include atmospheric entries at very high velocities or into an atmosphere with highly radiative constituents. The effects of gas radiation in the shock layer and wake flows may become significant at such flight conditions. Hence an accurate computational fluid dynamics analysis of these flows requires the energy transport by radiation using CFD software's (ICEM CFD, CFX-PRE, CFX-SOLVER, and CFX-POST). Therefore, have to conduct Eddy dissipation transport simulations to study the effects of Emission turbulent-radiation interaction over the capsule in hypersonic turbulent boundary layers, at peak heating condition during reentry. Furthermore, coupling between the ablation products from the surface of the vehicle and the high temperature gas can have a major effect on the heat load experienced by the capsule. The simulation will be conducted with different shapes of capsule and also with effect of ablation material on radiative heating by using different ablative materials (SiC, PICA, and AVCOAT). Numerical simulations based on computational fluid dynamics (CFD) demonstrate a guideline for selecting parameters during re-entry of capsule and help to find out the best materials for the construction of re-entry vehicle. The flow parameters and heat transfer characteristics investigated for all capsule configurations and results have to be extracted.

Keywords – Re-entry capsule, Ablative materials, CFD, Turbulence, Radiation Effect

I. INTRODUCTION

A re-entry capsule is the portion of a spacecraft which returns to Earth following a space flight. The shape is determined partly by aerodynamics; a capsule is aerodynamically stable falling blunt end first, which allows only the blunt end to require a heat shield for atmospheric reentry. Its shape has also been compared to that of an old-fashioned automobile's headlight. A manned capsule contains the spacecraft's instrument panel, limited storage space, and seats for crew members. Because a capsule shape has little aerodynamic lift, the final descent is via parachute, either coming to rest on land, at sea, or by active capture by another aircraft. In contrast, the development of space plane reentry vehicles attempts to provide a more flexible reentry profile.

The simplest axisymmetric shape is the sphere or spherical section. This can either be a complete sphere or a spherical section fore body with a converging conical after body. The aerodynamics of a sphere or spherical section is easy to model analytically using Newtonian impact theory

Pure spheres have no lift. However, by flying at an angle of attack, a spherical section has modest aerodynamic lift thus providing some cross-range capability and widening its entry corridor. In the late 1950s and early 1960s, high-speed computers were not yet available and computational fluid dynamics was still embryonic. Because the spherical section was amenable to closed-form analysis, that geometry became the default for conservative design. Consequently, manned capsules of that era re based upon the spherical section

The sphere-cone is a spherical section with a frustum or blunted cone attached. The sphere-cone's dynamic stability is typically better than that of a spherical section. With a sufficiently small half-angle and properly placed center of mass, a sphere-cone can provide aerodynamic stability from Keplerian entry to surface impact.

Reconnaissance satellite RVs (recovery vehicles) also used a sphere-cone shape and were the first American example of a non-munitions entry vehicle (Discoverer-I, launched on 28 February 1959). The sphere-cone was later used for space exploration missions to other celestial bodies or for return from open space; e.g., Stardust probe. Unlike with military RVs, the advantage of the blunt body's lower TPS mass remained with space exploration entry vehicles like the Galileo Probe with a half angle of 45° or the Viking aero shell with a half angle of 70°. Space exploration sphere-cone entry vehicles have landed on the surface or entered the atmospheres of Mars, Venus, Jupiter and Titan.

The biconic is a sphere-cone with an additional frustum attached. The biconic offers a significantly improved L/D ratio. A biconic designed for Mars aero capture typically has an L/D of approximately 1.0 compared to an L/D of

0.368 for the Apollo-CM. The higher L/D makes a biconic shape better suited for transporting people to Mars due to the lower peak deceleration. Arguably, the most significant biconic ever flown was the Advanced Maneuverable Reentry Vehicle (AMRV).

Non-axisymmetric shapes have been used for manned entry vehicles. One example is the winged orbit vehicle that uses a delta wing for maneuvering during descent much like a conventional glider. This approach has been used by the American Space Shuttle and the Soviet Buran. The lifting body is another entry vehicle geometry and was used with the X-23 PRIME (Precision Recovery Including Maneuvering Entry) vehicle.

SLA in SLA-561V stands for super light-weight ablator. SLA-561V is a proprietary ablative made by Lockheed Martin that has been used as the primary TPS material on all of the 70° sphere-cone entry vehicles sent by NASA to Mars other than the Mars Science Laboratory (MSL). SLA-561V begins significant ablation at a heat flux of approximately 110 W/cm², but will fail for heat fluxes greater than 300 W/cm².

Phenolic impregnated carbon ablator (PICA), a carbon fiber perform impregnated in phenolic resin, PICA is a modern TPS material and has the advantages of low density (much lighter than carbon phenolic) coupled with efficient ablative capability at high heat flux. It is a good choice for ablative applications such as high-peak-heating conditions found on sample-return missions or lunar-return missions. PICA's thermal conductivity is lower than other high-heat-flux ablative materials, such as conventional carbon phenolics.

An improved and easier to manufacture version called PICA-X was developed by SpaceX in 2006-2010 for the Dragon space capsule. The first re-entry test of a PICA-X heat shield was on the Dragon C1 mission on 8 December 2010. The PICA-X heat shield was designed, developed and fully qualified by a small team of only a dozen engineers and technicians in less than four years. PICA-X is ten times less expensive to manufacture than the NASA PICA heat shield material.

AVCOAT is a NASA-specified ablative heat shield, a glass-filled epoxy-novolac system. NASA originally used it for the Apollo capsule and then utilized the material for its next-generation beyond low Earth-orbit Orion spacecraft. The AVCOAT to be used on Orion has been reformulated to meet environmental legislation that has been passed since the end of Apollo.

II. ICEM CFD GEOMETRY AND MESH REPORT

The geometry of the reentry capsule is quite complex and the solid modeling is carried by ICEM CFD modeling tools. The dimensions are taken for the reentry capsule as from the base paper. The solid model was drawn in ICEM CFD by the help of design parameters of the reentry capsule will be shown in following tables. The model of the reentry capsule is modified slightly to do the flow analysis. Here the analysis the flow over the reentry capsule so requires the flow domain for the flow analysis. Therefore for flow analysis, a flow domain is created as for the dimensions required. Here creating the cylindrical shape domain with diameter 4L and length 11L, where L is the length of the reentry capsule. Before starting the mesh need to create the boundary layer around the reentry capsule body.

And then mesh the faces of the body by using unstructured mesh. To create 3D mesh of the domain the tetrahedral elements are used. Check the mesh of the domain for convergence. In this the flow domain selected as AIR for Outer region and SOLID for reentry capsule region. And the flow boundary is selected as INLET, OUTLET, and OUTER WALL for the outer region and WALL for the reentry capsule. The basic geometry, domain structure, meshed structured will be shown in following figures.

For aerodynamic analysis, four cases of capsules shapes and corresponding design parameters are taken from base paper and their parameters will be shown in table.

Four cases:

1. Mach number-10, AOA-0
2. Mach number-10, AOA-10
3. Mach number-12, AOA-0
4. Mach number-10, AOA-28

Table I Model configuration of case1

MODEL CONFIGURATION	DIMENSION
Total height	3.8m
Spheric Diameter	5m
Nose angle	33 deg
Frusted cone slant height	2.6m
Biconic cone height	0.8m
Frusted edge length	2.8m
Biconic base length	1.4m
Blunt body radius	0.4m

CASE 1) MACH 10 AOA 0:

Herewith, first draw the geometrical diagram which taken dimensions from the design configuration table. And have to convert the geometrical diagram into three dimensional objects in ICEM CFD.

Defining the domain with above mentioned dimension which surrounding the capsule which call as air domain and inside capsule which call as solid as shown in following figures. After using unstructured mesh generates with trihedral, have to converts the cylindrical domain into the meshed structure and get corresponding elements and nodes from the meshed parts as shown in following tables Furthermore, have to show the design geometry which we get from base paper with their configuration and appropriate domain and mesh diagram which got from ICEM CFD.

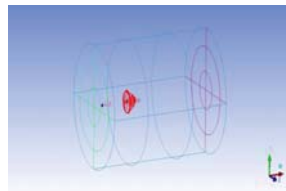


Fig 1 Domain Structure of Case 1 Capsule

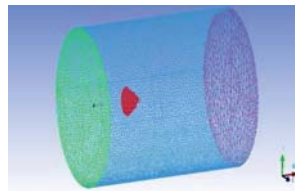


Fig 2 Meshed Structure of Case 1 Capsule

Subsequently, have got the meshed structure; the file is imported to CFX-PRE in that have to apply all boundary conditions values by using Eddy viscosity transport Equation to study the turbulence effects over the capsule which is covered by high ablative material for heat resistance. Here, have got the subsequent meshed details from the software and mentioned in the following table

CASE 2) MACH 10 AOA 10:

Herewith, first draw the geometrical diagram which taken dimensions from the design configuration table. And have to convert the geometrical diagram into three dimensional objects in ICEM CFD.

Defining the domain with above mentioned dimension which surrounding the capsule which call as air domain and inside capsule which call as solid as shown in following figures. After using unstructured mesh generates with trihedral, have to converts the cylindrical domain into the meshed structure and get corresponding elements and nodes from the meshed parts as shown in following tables Furthermore, have to show the design geometry which we get from base paper with their configuration and appropriate domain and mesh diagram which got from ICEM CFD.

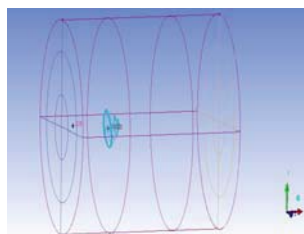


Fig 3 Domain Structure 2 of Case 2 Capsule

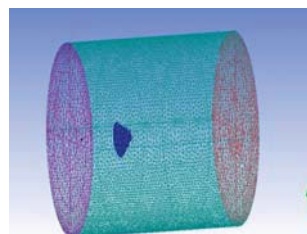


Fig 4 Meshed Structure of Case 2 Capsule

Subsequently, have got the meshed structure; the file is imported to CFX-PRE in that have to apply all boundary conditions values by using Eddy viscosity transport Equation to study the turbulence effects over the

capsule which is covered by high ablative material for heat resistance. Here, have got the subsequent meshed details from the software and mentioned in the following table

CASE 3) MACH 12 AOA 0:

Herewith, first draw the geometrical diagram which taken dimensions from the design configuration table. And have to convert the geometrical diagram into three dimensional objects in ICEM CFD. Defining the domain with above mentioned dimension which surrounding the capsule which call as air domain and inside capsule which call as solid as shown in following figures. After using unstructured mesh generates with trihedral, have to converts the cylindrical domain into the meshed structure and get corresponding elements and nodes from the meshed parts as shown in following tables Furthermore, have to show the design geometry which we get from base paper with their configuration and appropriate domain and mesh diagram which got from ICEM CFD.

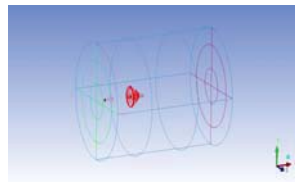


Fig 5 Domain Structure of Case 3 Capsule

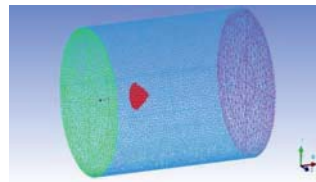


Fig 6 Meshed Structure of Case 3 Capsule

Subsequently, have got the meshed structure; the file is imported to CFX-PRE in that have to apply all boundary conditions values by using Eddy viscosity transport Equation to study the turbulence effects over the capsule which is covered by high ablative material for heat resistance. Here, have got the subsequent meshed details from the software and mentioned in the following table

CASE 4) MACH 12 AOA 28:

Herewith, first draw the geometrical diagram which taken dimensions from the design configuration table. And have to convert the geometrical diagram into three dimensional objects in ICEM CFD. Defining the domain with above mentioned dimension which surrounding the capsule which call as air domain and inside capsule which call as solid as shown in following figures. After using unstructured mesh generates with trihedral, have to converts the cylindrical domain into the meshed structure and get corresponding elements and nodes from the meshed parts as shown in following tables Furthermore, have to show the design geometry which we get from base paper with their configuration and appropriate domain and mesh diagram which got from ICEM CFD.

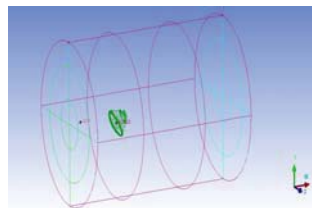


Fig 7 Domain Structure of Case 4 Capsule

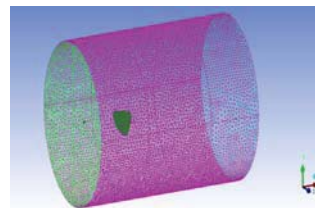


Fig 8 Meshed Structure of Case 4 Capsule

Subsequently, have got the meshed structure; the file is imported to CFX-PRE in that have to apply all boundary conditions values by using Eddy viscosity transport Equation to study the turbulence effects over the capsule which is covered by high ablative material for heat resistance. Here, have got the subsequent meshed details from the software and mentioned in the following table

Table II Mesh Information for Case 4 Capsule

Domain	Nodes	Elements
air	72255	362635
solid	30406	146102
All Domains	102661	508737

III. IMPLEMENTATION

For each case will have to treat analysis with three high ablative materials which mentioned as follows. Since, the boundary conditions which have accumulate from base paper will be apply for all cases and it will be tabulated as follows And will have to show flow characteristics values and radiative heat loading properties values over the capsule and also finally which will show that which ablative material will be good for shielding by analyzing report.

After the mesh of the reentry capsule in ICEM CFD then it is imported to CFX-PRE software for the flow analysis with following mentioned boundary conditions. After importing of the mesh file into the CFX-SOLVER are checking the mesh for the accurate solution and applying accurate values for domains and boundaries. Then the CFX-SOLVER file is imported to CFX-POST-solver, which it solving the corresponding iterations by using finite element analysis. And can see the all types of flow characteristics and corresponding results will have to be categorized in CFX-POST after imported file from the solver. For each case will have to treat analysis with three high ablative materials mentioned as follows. And finally which will show that which ablative material will be good for shielding by analyzing report.

From the studies of relating paper, the three resin materials have very low thermal conductivity and have good ablative properties such as Silicon, Phenolic and epoxy resins which are mainly using for supersonic and hypersonic reentry vehicles. In view of the fact that the suitable ablative materials such as SIC, PICA, AVCOAT which have the corresponding resins good proportionality. So, here from the basic explanation had taken the three materials and will have to analyze the flow properties with these three ablative materials.

1. SILICON CARBIDE
2. PICA
3. AVCOAT

Table III Boundary Conditions for all cases

Domain	Air	Basic settings	
		Location	Air
		Domain type	Fluid domain
		Option	Material library
		Material	Air ideal gas
		Reference pressure	1 Pascal
		Heat transfer	Total energy
		Turbulence	Eddy viscosity Transport equation
		Wall function	High speed heat transfer function
	Solid	Basic settings	
		Location	Solid
		Domain type	Solid domain
		Option	Material library

		Material	Siliconcarbide, Pica,Avcoat
		Heat transfer	Thermal energy
Boundary	Inlet- Mach 10	Boundary type	Inlet
		Flow regime	Supersonic
		Normal speed	3843.12m/s
		Static Pressure	32.78 Pascal
		Total Temperature	7607.1k
		Turbulence	Medium intensity
	Inlet- Mach 12	Normal speed	3297.7 m/s
		Static Pressure	79.78 Pascal
		Total Temperature	5683.6 k
		Turbulence	Medium intensity
	Outlet	Boundary type	Outlet
		Flow regime	Supersonic
	Wall	Boundary type	Outer wall
		Wall	Free slip wall
		Heat transfer	Adiabatic
	Interface	Interface type	Fluid solid
		Model	General connection
	Reaction	Material list	N,N2,NO,O,O2,H2
		Combustion Type	Finite chemistry & Eddy Dissipation
		Thermal condition	Local Temperature
		Mass Fraction	1

Table IV Material properties of heat ablative materials

Si.No	Properties	SIC	PICA	AVCOAT
1	Resins	Silicon carbide	Phenolic carbon	Epoxy resin
2	Density	3.1 g cm ⁻³	1.0413 g cm ⁻³	0.51 g cm ⁻³
3	Molar mass	40.11 g mol ⁻¹	34.14 g mol ⁻¹	21.81 g mol ⁻¹
4	Specific heat capacity	750 J kg ⁻¹ K ⁻¹	1021 J kg ⁻¹ K ⁻¹	1327 J kg ⁻¹ K ⁻¹
5	Thermal conductivity	120 W m ⁻¹ K ⁻¹	142.7 W m ⁻¹ K ⁻¹	238.4 W m ⁻¹ K ⁻¹

Aerodynamic Analysis of 4 cases with Silicon Carbide:

Subsequently, the file is imported to CFX-PRE. In that have to apply all boundary conditions values by using Eddy viscosity transport Equation to study the Turbulence effects over the capsule which is covered by high ablative material Silicon Carbide for heat resistance.

Here, will have to analyze the all cases with high ablative material silicon carbide by applying ideal boundary conditions in CFX-POST-PRE and get the report from the software which will be indicated as follows.

After get the successfully solved file from the CFX, have to see the consequent flow characteristics with respect to contours and streamline path of given boundary flow and have to obtain the exacting data's from the analysis. The ideal values have to be tabulated from the flow characteristic values

Table V Flow characteristics of Case 1 with SiC

Si.No	Flow Characteristics	Values
1	Pressure	1.578*10 ⁴ Pascal
2	Temperature	5.651*10 ³ K
3	Velocity	3.187*10 ³ m/s
4	Total Temperature	5.745*10 ³ K
5	Total Pressure	4.649*10 ⁶ Pascal
6	Mach Number	10

Table VI Flow characteristics of Case 2 with SiC

Si.No	Flow Characteristics	Values
1	Pressure	1.450*10 ⁴ Pascal
2	Temperature	5.586*10 ³ K
3	Velocity	3.221*10 ³ m/s
4	Total Temperature	5.802*10 ³ K
5	Total Pressure	9.261*10 ⁶ Pascal
6	Mach Number	10

Table VII Flow characteristics of Case 3 with SiC

SI.NO	Flow Characteristics	VALUES
1	Pressure	9.938*10 ³ Pascal
2	Temperature	7.613*10 ³ K
3	Velocity	3.744*10 ³ m/s
4	Total Temperature	7.755*10 ³ K
5	Total Pressure	1.015*10 ⁷ Pascal
6	Mach Number	12

Table VIII Flow characteristics of case 4 with SiC

Si.No	Flow Characteristics	Values
1	Pressure	8.723×10^3 Pascal
2	Temperature	7.563×10^3 K
3	Velocity	3.731×10^3 m/s
4	Total Temperature	7.819×10^3 K
5	Total Pressure	1.042×10^7 Pascal
6	Mach Number	12

Aerothermodynamic Analysis of 4 cases with SiC:

The mixture of gases such as (O, N, NO, O₂, and N₂) are involved in atmospheric region with cylindrical and three-dimensional computations for both perfect and chemically reacting-gas approximation have been performed for the free stream conditions. The far field is assumed to be made up of 79% of molecular nitrogen (N₂) and 21% of molecular oxygen (O₂). Moreover, for a more accurate assessment of the reliability of present results, several analysis have been made with results from simplified solution methods and will have to result of radiative heat loading over the capsule and corresponding chemical mass fraction effect on the capsule. Here silicon carbide as high ablative material with their properties for reactive analysis is used.

Here, will have to show the analysis report of mass fraction effect on the reentry vehicle and radiative properties over the capsule with respect to corresponding mach numbers and ablative materials which covered over the vehicle.

The corresponding reaction values of radiative heat loading on reentry capsule are tabulated as follows.

Table IX Reaction properties of Case 1 with SiC

Si No	Reaction Properties	Values
1	Radiation Intensity	9.954×10^4
2	Incident Radiation	1.215×10^6 W/m ²
3	Turbulence Effects Eddy	5.272×10^9 m ² /s ³
4	Turbulence Effects Kinetic	7.282×10^5 m ² /s ²

Table X Reaction properties of Case 2 with SiC

Si No	Reaction Properties	Values
1	Radiation Intensity	1.417×10^5 ws/ m ² r
2	Incident Radiation	1.817×10^6 w/m ²
3	Turbulence Eddy	4.222×10^9 m ² /s ³
4	Turbulence Kinetic	7.421×10^5 m ² /s ²

Table XI Reaction properties of Case 3 with SiC

Si No	Reaction Properties	Values
1	Radiation Intensity	6.530×10^4 ws/ m ² r
2	Incident Radiation	8.310×10^5 w/m ²
3	Turbulence eddy	9.178×10^9 m ² /s ³
4	Turbulence Kinetic	9.161×10^5 m ² /s ²

Table XII Reaction properties of case 4 with SiC

Si No	Reaction Properties	Values
1	Radiation Intensity	6.428×10^4 ws/m ² r
2	Incident Radiation	8.078×10^5 w/m ²
3	Turbulence Eddy	1.675×10^{10} m ² /s ³
4	Turbulence Kinetic	1.096×10^6 m ² /s ²

Aerodynamic Analysis of 4 cases with PICA:

Subsequently, the file is imported to CFX-PRE. In that have to apply all boundary conditions values by using Eddy viscosity transport Equation to study the Turbulence effects over the capsule which is covered by high ablative material Silicon Carbide for heat resistance.

Here, will have to analyze the all cases with high ablative material silicon carbide by applying ideal boundary conditions in CFX-POST-PRE and get the report from the software which will be indicated as follows.

After get the successfully solved file from the CFX, have to see the consequent flow characteristics with respect to contours and streamline path of given boundary flows and have to obtain the exacting data's from the analysis.

The ideal values have to be tabulated from the flow characteristic values

Table XIII Flow characteristics of Case 1 with PICA

Si.No	Flow Characteristics	Values
1	Pressure	$1.437 \cdot 10^4$ Pascal
2	Temperature	$5.537 \cdot 10^3$ K
3	Velocity	$3.270 \cdot 10^3$ m/s
4	Total Temperature	$5.712 \cdot 10^3$ K
5	Total Pressure	$4.669 \cdot 10^6$ Pascal
6	Mach Number	10

Table XIV Flow characteristics of Case 2 with PICA

Si.No	Flow Characteristics	Values
1	Pressure	$1.236 \cdot 10^4$ Pascal
2	Temperature	$5.507 \cdot 10^3$ K
3	Velocity	$3.268 \cdot 10^3$ m/s
4	Total Temperature	$5.802 \cdot 10^3$ K
5	Total Pressure	$4.374 \cdot 10^7$ Pascal
6	Mach Number	10

Table XV Flow characteristics of case 3 with PICA

Si.No	Flow Characteristics	Values
1	Pressure	$9.672 \cdot 10^3$ Pascal
2	Temperature	$7.563 \cdot 10^3$ K
3	Velocity	$3.829 \cdot 10^3$ m/s
4	Total Temperature	$7.796 \cdot 10^3$ K
5	Total Pressure	$9.473 \cdot 10^6$ Pascal
6	Mach Number	12

Table XVI Flow characteristics of case 4 with PICA

Si.No	Flow Characteristics	Values
1	Pressure	$7.345 \cdot 10^3$ Pascal
2	Temperature	$7.441 \cdot 10^3$ K
3	Velocity	$3.828 \cdot 10^3$ m/s
4	Total Temperature	$7.742 \cdot 10^3$ K
5	Total Pressure	$9.063 \cdot 10^6$ Pascal
6	Mach Number	12

Aerothermodynamic Analysis of 4 cases with PICA:

The mixture of gases such as (O, N, NO, O₂, and N₂) are involved in atmospheric region with cylindrical and three-dimensional computations for both perfect and chemically reacting-gas approximation have been performed for the free stream conditions. The far field is assumed to be made up of 79% of molecular nitrogen (N₂) and 21% of molecular oxygen (O₂). Moreover, for a more accurate assessment of the reliability of present results, several analysis have been made with results from simplified solution methods and will have to result of radiative heat loading over the capsule and corresponding chemical mass fraction effect on the capsule. Here are using Phenolic-carbon resin PICA as high ablative material with their properties for reactive analysis.

Here, will have to show the analysis report of mass fraction effect on the reentry vehicle and radiative properties over the capsule with respect to corresponding mach numbers and ablative materials which covered over the vehicle.

The corresponding reaction values of radiative heat loading on reentry capsule are tabulated as follows

Table XVII Reaction properties contour of Case 1 with PICA

Si No	Reaction Properties	Values
1	Radiation effects Intensity	$1.394 \cdot 10^5$ Ws/m ² r
2	Incident Radiation effects	$1.752 \cdot 10^6$ w/m ²
3	Turbulence effects Eddy Dissipation	$4.769 \cdot 10^9$ m ² /s ³
4	Turbulence effects Kinetic Energy	$7.553 \cdot 10^5$ m ² /s ²

Table XVIII Reaction properties of Case 2 with PICA

Si No	Reaction Properties	Values
1	Radiation Intensity	$1.264 \cdot 10^5$ ws/ m ² r
2	Incident Radiation	$1.655 \cdot 10^6$ w/m ²
3	Turbulence Eddy Dissipation	$4.008 \cdot 10^9$ m ² /s ³
4	Turbulence Kinetic Energy	$7.302 \cdot 10^5$ m ² /s ²

Table XIX Reaction properties of case 3 with PICA

Si No	Reaction Properties	Values
1	Radiation Intensity	$6.528 \cdot 10^4$ ws/
2	Incident Radiation	$8.289 \cdot 10^5$ w/m ²
3	Turbulence Eddy Dissipation	$8.851 \cdot 10^9$ m ² /s ³
4	Turbulence Kinetic Energy	$8.961 \cdot 10^5$ m ² /s ²

Table XX Reaction properties of case 4 with PICA

Si No	Reaction Properties	Values
1	Radiation Intensity	$6.421 \cdot 10^4$ ws/m ² r
2	Incident Radiation	$8.069 \cdot 10^5$ w/m ²
3	Turbulence Eddy Dissipation	$1.631 \cdot 10^{10}$ m ² /s ³
4	Turbulence Kinetic Energy	$1.032 \cdot 10^6$ m ² /s ²

Aerodynamic Analysis of 4 cases with AVCOAT:

Subsequently, the file is imported to CFX-PRE. In that have to apply all boundary conditions values by using Eddy viscosity transport Equation to study the Turbulence effects over the capsule which is covered by high ablative material Silicon Carbide for heat resistance.

Here, will have to analyze the all cases with high ablative material silicon carbide by applying ideal boundary conditions in CFX-POST-PRE and get the report from the software which will be indicated as follows.

Flow Characteristics of Case 1 with AVCOAT:

After get the successfully solved file from the CFX, have to see the consequent flow characteristics with respect to contours and streamline path of given boundary flows and have to obtain the exacting data's from the analysis.

The ideal values have to be tabulated from the flow characteristic values

Table XXI Flow characteristics Case 1 with AVCOAT

Si.No	Flow Characteristics	Values
1	Pressure	$1.360 \cdot 10^4$ Pascal
2	Temperature	$5.244 \cdot 10^3$ K
3	Velocity	$3.303 \cdot 10^3$ m/s
4	Total Temperature	$5.490 \cdot 10^3$ K
5	Total Pressure	$4.216 \cdot 10^6$ Pascal
6	Mach Number	10

Table XXII Flow characteristics of Case 2 with AVCOAT

Si.No	Flow Characteristics	Values
1	Pressure	$1.286 \cdot 10^4$ Pascal
2	Temperature	$5.453 \cdot 10^3$ K
3	Velocity	$3.360 \cdot 10^3$ m/s
4	Total Temperature	$5.507 \cdot 10^3$ K
5	Total Pressure	$4.374 \cdot 10^7$ Pascal
6	Mach Number	10

Table XXIII Flow characteristics of case 3 with AVCOAT

SI.NO	Flow Characteristics	VALUES
1	Pressure	$9.088 \cdot 10^3$ Pascal
2	Temperature	$7.365 \cdot 10^3$ K
3	Velocity	$3.848 \cdot 10^3$ m/s
4	Total Temperature	$7.882 \cdot 10^3$ K
5	Total Pressure	$9.220 \cdot 10^6$ Pascal
6	Mach Number	12

Table XXIV Flow characteristics of case 4 with AVCOAT

Si.No	Flow Characteristics	Values
1	Pressure	$6.972 \cdot 10^3$ Pascal
2	Temperature	$7.190 \cdot 10^3$ K
3	Velocity	$3.848 \cdot 10^3$ m/s
4	Total Temperature	$7.727 \cdot 10^3$ K
5	Total Pressure	$8.602 \cdot 10^6$ Pascal
6	Mach Number	12

Aerothermodynamic Analysis of 4 cases with AVCOAT:

The mixture of gases such as (O, N, NO, O₂, and N₂) are involved in atmospheric region with cylindrical and three-dimensional computations for both perfect and chemically reacting-gas approximation have been performed for the free stream conditions. The far field is assumed to be made up of 79% of molecular nitrogen (N₂) and 21% of molecular oxygen (O₂). Moreover, for a more accurate assessment of the reliability of present results, several analysis have been made with results from simplified solution methods and will have to result of radiative heat loading over the capsule and corresponding chemical mass fraction effect on the capsule. Here are using Epoxy Novolac resin AVCOAT as high ablative material with their properties for reactive analysis.

Here, will have to show the analysis report of mass fraction effect on the reentry vehicle and radiative properties over the capsule with respect to corresponding mach numbers and ablative materials which covered over the vehicle.

The corresponding reaction values of radiative heat loading on reentry capsule are tabulated as follows

Table XXV Reaction properties Of Case 1 With AVCOAT

Si No	Reaction Properties	Values
1	Radiation effects Intensity	$1.855 \cdot 10^5$ ws/m ² r
2	Incident Radiation effects	$2.331 \cdot 10^6$ w/m ²
3	Turbulence Eddy Dissipation	$4.577 \cdot 10^9$ m ² /s ³
4	Turbulence Kinetic Energy	$8.126 \cdot 10^5$ m ² /s ²

Table XXVI Reaction properties of Case 2 with AVCOAT

Si No	Reaction Properties	Values
1	Radiation Intensity	$9.323 \cdot 10^4$ ws/ m ² r
2	Incident Radiation	$1.205 \cdot 10^6$ w/m ²
3	Turbulence Eddy Dissipation	$3.926 \cdot 10^9$ m ² /s ³
4	Turbulence Kinetic Energy	$6.974 \cdot 10^5$ m ² /s ²

Table XXVII Reaction properties of case 3 with AVCOAT

Si No	Reaction Properties	Values
1	Radiation Intensity	$6.516 \cdot 10^4$ ws/m ² r
2	Incident Radiation	$8.147 \cdot 10^5$ w/m ²
3	Turbulence eddy Discipation	$8.844 \cdot 10^9$ m ² /s ³
5	Turbulence Kinetic Energy	$8.844 \cdot 10^5$ m ² /s ²

Table XXVIII Reaction properties of case 4 with AVCOAT

Si No	Reaction Properties	Values
1	Radiation Intensity	$6.332 \cdot 10^4$ ws/m ² r
2	Incident Radiation	$7.855 \cdot 10^5$ w/m ²
3	Turbulence Eddy Dissipation	$1.567 \cdot 10^{10}$ m ² /s ³
4	Turbulence Kinetic Energy	$1.008 \cdot 10^6$ m ² /s ²

Grid Independence Study and Validation:

Computations have been carried out on multi block structured grids generated with the tool ICEM-CFD. Each grid is tailored to account for the specific flow conditions of each case reported. Each mesh contains 32 blocks, for an overall number of about 750,000 cells (half-body only, since no sideslip velocity has been accounted for). In particular, the mesh was initially generated algebraically and then adapted as the solution evolved, aligning the grid with the bow shock and clustering points in the boundary layer. This reduces the spurious oscillations in the

stagnation area that are often observed in hypersonic flows, especially for large blunt-body flow field computations. The distribution of surface grid points was dictated by the level of resolution desired in various areas of the vehicle, such as the stagnation region and base fillet, according to the computational aims. The value of the grid spacing near the wall was found to be on the order of 10^{-6} m to accurately predict heat transfer at the vehicle surface. Further, the number of grid points in the shoulder region was large enough to capture the rapid expansion that the flow experienced locally and to then accurately predict flow separation and the angle of the resulting shear layer. There are also sufficient points in the separated-flow region to resolve the vortical structure at the beginning of the wake flow.

Therefore, the validations have got by locating the polyline from top centre to the bottom centre line of the capsule and have got flow contours graph with respect to s/R_b which s refer to curve length, and R_b refer to capsule shoulder radius and it simply indicate to centre line of the capsule. The variation of shock and expansion characteristics over the capsule can be clearly seen from the Pressure co-efficient distribution over the capsule.

In this paper the computations have been carried out multi block unstructured grid generated with the tool ICEM CFD. The model of the reentry capsule is modified slightly to do the flow analysis. Here the analysis the flow over the reentry capsule so requires the domain for the flow analysis. Therefore for flow analysis, a domain is created as for the dimensions required. Here creating the cylindrical shape domain with diameter $4L$ and length $11L$, where L is the length of the reentry capsule. Before starting the mesh need to create the boundary layer around the reentry capsule body.

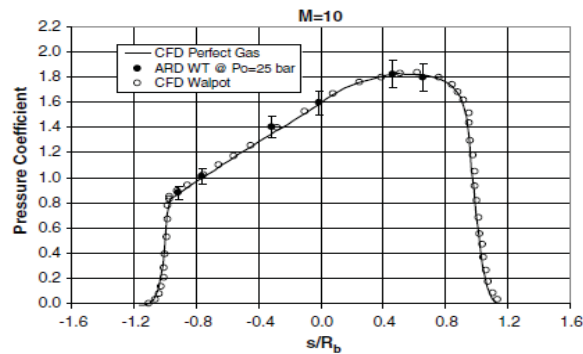


Fig 9 Pressure Co-efficient at forebody centerline

Creating 3D mesh of the domain the trihedral pave elements are used. Check the mesh of the domain for convergence. In this the flow domain selected as AIR for Outer region and SOLID for reentry capsule region. And the flow boundary is selected as INLET, OUTLET, and OUTER WALL for the outer region and WALL for the reentry capsule.

And lastly got the total number of elements and nodes with respect to air domain is 362635 and 72255. Similarly have got the total number of elements and nodes with respect to solid domain is 146102 and 30406. There are also sufficient points in the separated-flow region to resolve the vortical structure at the beginning of the wake flow.

Therefore, in this paper the validations have got by locating the polyline from top centre to the bottom centre line of the capsule and have got flow contours graph with respect to s/R_b which s refer to curve length, and R_b refer to capsule shoulder radius and it simply indicate to centre line of the capsule. The results obtained and validated report from all the analyses are compared in the chapter below. The variation of shock and expansion characteristics over the capsule can be clearly seen from the Pressure co-efficient distribution over the capsule.

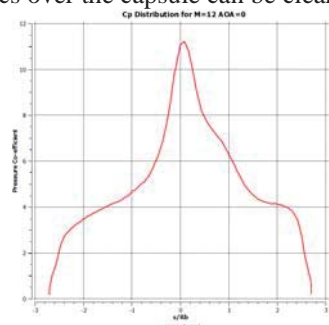


Fig10 Pressure distribution for Mach 12

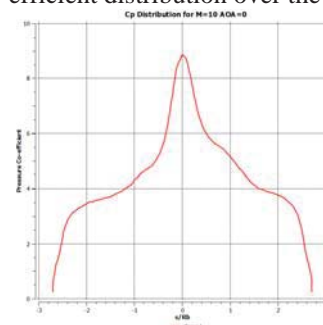


Fig11 Pressure distribution for Mach 10

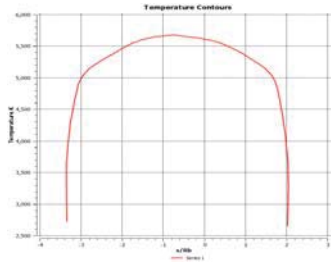


Fig12 Temperature contour

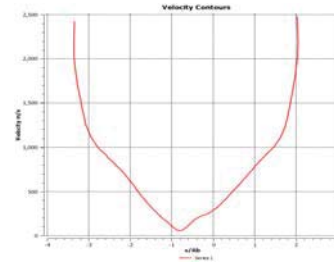


Fig 13 Velocity contour

IV.COMPARATIVE STUDIES AND CONCLUSION

Subsequently, validations was done with respect to the capsule grid independence and the results obtained and validated report from all the analyses are compared in the section below. And the corresponding flow characteristics such as pressure, temperature, and velocity during reentry have been compared for all cases. And also compared the values of the radiation and turbulence effects over the capsule at the time of reentry .The variation of shock and expansion characteristics over the capsule can be clearly seen from the Pressure co-efficient distribution over the capsule.

From the analysing report of flow characteristics, have been obtained the accurate value for each flow properties.Since, had compared all cases values with corresponding to proper flow properties values and had got which ablative material cases giving perfect values.The chart diagram had been used for comparison of all cases flow values with respect to suitable high ablative materials.

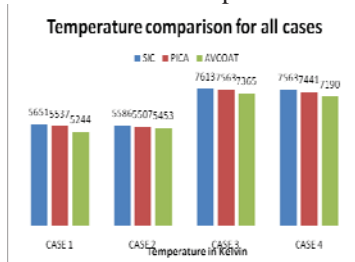


Fig 14 Temperature comparison for all cases

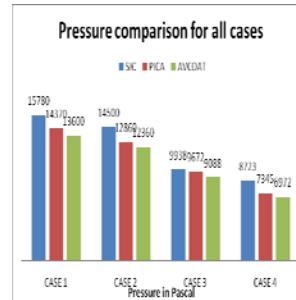


Fig 15 Pressure comparison for all cases

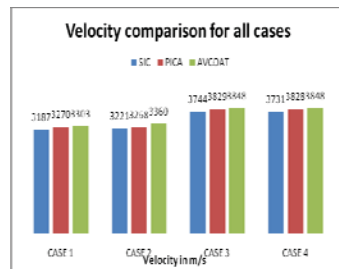


Fig 16 Velocity comparison for all cases

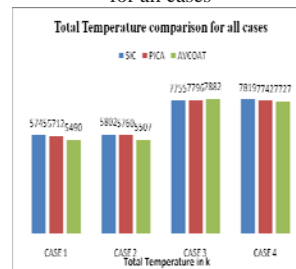


Fig 17 Total temperature comparison for all cases

After we analysed and compared flow characteristics values,had compared the values of radiative effects and turbulence effects over the reentry capsule with respect to mass fraction effects of the major elements which are present in the atmospheric air.Here, had compared the values by using chart diagram and finalising which one are giving ideal standards with respect to the high ablative materials which covered in different cases of capsules.

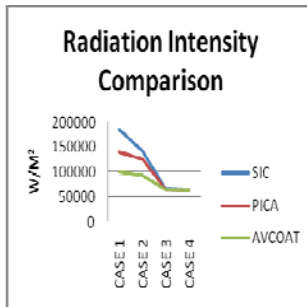


Fig 18 Comparison of radiation intensity

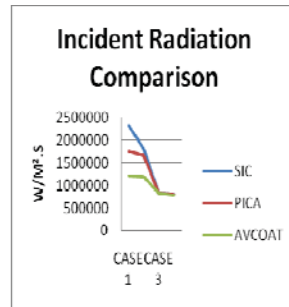


Fig 19 Comparison of incident radiation

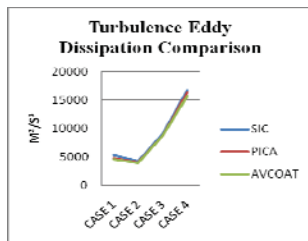


Fig 20 Comparison of turbulent eddy dissipation

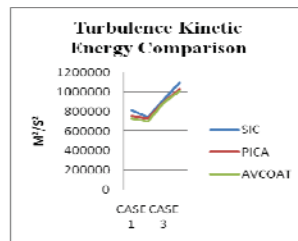


Fig 21 Comparison of turbulent kinetic energy

In this project, have analysed and studied about all types of cases which include different mach number with variable AOA of re-entry vehicle which covered by three different high ablative materials such as SiC, PICA, AVCOAT. And studied evidently about the turbulence effect over the capsule at hypersonic speed by using Eddy Dissipation Transport Simulation and have studied the effects of gas radiation in the shock layer and wake flows became significant at such flight conditions. Then got the corresponding flow characteristics values for each cases with respect to ablative materials. Further, have got the distinguishing values of radiative heat loading and turbulence effect on the capsule during re-entry from the consequence of mass fraction of elements which presented mostly in the atmospheric air with the capsule at hypersonic speed. Subsequently have compared all flow properties values and significance of radiative heat loading and turbulence effect values by using chart diagram. After comparing with the results, have concluded that AVCOAT is best suited for all sections of capsule for re-entry, as it has lower temperature effects than both ablative materials. At high Mach number of vehicle, velocity of flow increased and the pressure of the vehicle decreases drastically. At low Mach number of vehicle, there is an effect on vehicle skin will be corrodes by high temperature due to low Mach number of vehicle used. The reentry vehicle behaves differently at different mach numbers. In our future we strongly hope our studied about fluid dynamics over the re-entry vehicle will help us to do our higher studies and to get higher level job in national level fluid dynamics research industry.

REFERENCES

- [1] Antonio Viviani and Giuseppe Pezzella, "Computational Flow field Analysis over a Blunt-Body Reentry Vehicle", Journal Of Spacecraft And Rockets, Vol. 47, No. 2, March April 2010.
- [2] Antonio Viviani and Giuseppe Pezzella, "Analysis Of Thermo chemical Modeling and Surface Catalyticity In Space Vehicles Reentry", International Congress Of The Aeronautical Sciences Vol. 26, 2008.
- [3] Antonio Viviani and Giuseppe Pezzella "Dependence and Sensitivity on the Aero thermo chemical Model Of Atmospheric Reentry Trajectories", Progress in Flight Physics, Vol.3, 2012.
- [4] Peter A. Gnoffo, "A Perspective on Computational Aerothermodynamics at NASA", Australasian Fluid Mechanics Conference, Vol.16, December-2007.
- [5] Dr.B.Balakrishna, S. Venkateswarlu, and Dr P. Ravinder Reddy, "Flow Analysis of an Atmosphere Reentry Vehicle", International Journal of Engineering Research and Development, Vol.3, No-2PP.52-57, August-2012.
- [6] Xiang Li and Bao-Guo Wang, "CFD Prediction of Hypersonic Blunt-Cone Configurations of Multiple Cases", International Space Planes and Hypersonic Systems and Technologies Conference, Vol-16, 2009.
- [7] Tariq S. Najim, Amel M. Naji and Mahmood M. Barbooti, "Thermal and Ablative Properties of Ipn's and Composites of High Ortho Resole Resin and Difurfurylidene Acetone", Leonardo Electronic Journal of Practices and Technologies, Vol.13, December-2008.
- [8] Dr. James L. Pittman, "Hypersonic Project Fundamental Aeronautics Program", National Aeronautics and Space Administration, March-2012.

- [9] Antonio Viviani and Giuseppe Pezzella. "Computational Flow field Analysis of a Planetary Entry Vehicle", Journal of Spacecraft and Rockets, Vol. 47, No. 2, march - April 2008.
- [10] Gnoffo, P. A., Gupta, R. N., and Shinn, J., "Conservation Equations and Physical Models for Hypersonic Air Flows in Thermal and Chemical Non equilibrium," NASATP 2867, Feb. 1989.
- [11] Walpot, L., "Numerical Analysis of the ARD Capsule in S4 Wind Tunnel," Proceedings of the 4th European Symposium Aerothermodynamics for Space Applications, SP-487, ESA, Noordwijk, The Netherlands, March 2002.
- [12] Bertin, J. J., "The Effect of Protuberances, Cavities, and Angle of Attack on the Wind-Tunnel Pressures and Heat-Transfer Distribution for the Apollo Command Module," NASATM X-1243, 1966.
- [13] Crowder, R. S., and Moote, J. D., "Apollo Entry Aerodynamics," Journal of Spacecraft and Rockets, Vol. 6, No. 3, 1969, pp. 302–307.
- [14] Roncioni, P., Rufolo, G. C., Votta, R., and Marini, M., "An Extrapolation-to-Flight Methodology for Wind Tunnel Measurements Applied to the PRORA-USV FTB1 Vehicle," International Astronautical Congress Paper 06-D2.3.09, Valencia, Spain, 2– 6 October 2006.
- [15] Lees, L., "Laminar Heat Transfer over Blunt-Nosed Bodies at Hypersonic Speeds," Jet Propulsion Vol. 26, No. 4, 1956, pp. 259–269.
- [16] Donald L. Schmidt, "Ablation Materials", Pearson Education, 2nd edition, 2005, PP 23-135.